# Effect of Ball-milling Time on Particle Size of $Ca_3Co_4O_{9+\delta}$

**N. Prasoetsopha[1*], S. Pinitsoontorn[2], T. Kamwanna[2], K. Kurosaki[3] and S. Yamanaka[3]**

*[1]Materials Science and Nanotechnology Program, Faculty of Science, Khon Kaen University, Khon Kaen 40002, Thailand*
*[2]Department of Physics, Faculty of Science, Khon Kaen University, Khon Kaen 40002, Thailand*
*[3]Division of Sustainable Energy and Environment Engineering, Graduate School of Engineering, Osaka University, Suita, Osaka, 565-0871, Japan*

**Corresponding author. E-mail: butsciku@hotmail.com*

## ABSTRACT

***Thermoelectric (TE) materials can directly convert heat to electricity, or vice versa. The misfit-layered $Ca_3Co_4O_{9+\delta}$ is one of the most promising TE oxide materials, due to its high figure-of-merit (ZT) close to 1.0. In this study, polycrystalline $Ca_3Co_4O_{9+\delta}$ ceramics were prepared by a simple, thermal, hydro-decomposition method. The influence of ball-milling time on particle size was investigated. The ball-milling process used tungsten carbine balls with a diameter of 1.6 mm, a ball-per-powder ratio of 10:1, rotating speed of 300 rpm, milling time of 2.5 - 20 h and acetone as the dispersion media. The crystal structure and crystallite size were characterized by X-ray diffraction. The single phase of every cobaltite sample was obtained. The particle size and morphology were observed by a field emission scanning electron microscope (FESEM). The particle size was observed to be about 1 μm before ball milling, and was reduced down to 200 nm after milling. The ball-milled particles were fabricated to form bulk ceramics using a spark plasma sintering (SPS) technique. However, second phases were found for the bulk ceramics. The Seebeck coefficient, resistivity and thermal conductivity of the milled sample was higher than that of the unmilled sample. The highest ZT values of the unmilled and milled samples were 0.11 and 0.10, respectively, at 773 K.***

**Keywords:** $Ca_3Co_4O_9$, Ball mill, Thermoelectric, Thermal hydro-decomposition

## INTRODUCTION

Thermoelectric (TE) materials can directly convert heat to electricity, or vice versa. Recently, many researchers have been attracted to TE materials, because they are noiseless, have no moving parts and are environmentally friendly. Several kinds of TE materials, including alloys, skutterudite and oxides have been investigated (Koumoto et al., 2006; Tritt and Subramanian, 2006; Ohta et al. 2008; Snyder and Toberer, 2008). Thermoelectric efficiency is defined

as a dimensionless figure-of-merit, $ZT = S^2T/\rho\kappa$, where *Z, T, S,* $\rho$ and $\kappa$ are the figure-of-merit, absolute temperature, Seebeck coefficient (or so called thermopower), electrical resistivity and total thermal conductivity, respectively. In practice, $ZT \geq 1.0$ is required. The dependence of three parameters – *S,* $\rho$, and $\kappa$ – makes it difficult to improve TE properties. However, considerable research has attempted to solve this challenging problem by many means; for example, doping with other elements (Pei et al., 2008; Liu et al., 2009; Wang et al., 2010), improving the fabrication process (Yuankui et al., 2010; Noudem et al., 2012) or making composites (Xiang et al., 2008).

The misfit-layered $Ca_3Co_4O_{9+\delta}$ is one of the most promising TE oxide materials due to its non-toxicity, high oxidation resistance, high Seebeck coefficient and low resistivity (Masset et al., 2000). The single crystal $Ca_3Co_4O_{9+\delta}$ showed the highest *ZT* of 0.87 at 973 K (Shikano and Funahashi, 2003). Although the single crystal provides a high density and good TE properties, it is very difficult to fabricate in a large quantity. Therefore, polycrystalline $Ca_3Co_4O_{9+\delta}$, though having a lower *ZT* than the single crystal counterpart, is a more suitable choice for practical use. One of the methods to improve TE properties of polycrystalline $Ca_3Co_4O_{9+\delta}$ is by doping with other elements. Partially substitution of several metals, either for Ca or Co, have been investigated; for example, Ga (Nong et al., 2011), Ti (Xu et al., 2010), Fe (Liu et al., 2006; Wang et al., 2010), Cu (Wang et al., 2010), Mn (Wang et al., 2010) and Y (Liu et al., 2009).

Furthermore, nanostructures are a novel approach to enhance TE properties, due to a reduction of thermal conductivity. It is hypothesized that nanostructures can scatter phonon strongly so that they can reduce the total thermal conductivity. Yin et al. (2010) compared thermoelectric properties of $Ca_3Co_4O_{9+\delta}$ between the nanocrystals prepared by electrospinning and the conventional crystals prepared by a sol-gel method. TE properties were enhanced by nanocrystalline particles (Yin et al., 2010).

Ball milling is one of the processes that can reduce particle size or create nanostructure. Thus, it is a promising method to improve the thermoelectric properties of the sample. In this work, polycrystalline $Ca_3Co_4O_{9+\delta}$ were synthesized by a simple thermal hydro-decomposition method and subjected to the ball-milling process to decrease the particle size. The effect of ball-milling time on particle size was investigated. Then, the TE properties of bulk ceramics, prepared from unmilled and milled samples by a spark plasma sintering, were studied.

## MATERIALS AND METHODS

Misfit-layered $Ca_3Co_4O_{9+\delta}$ polycrystals were synthesized by a simple, thermal, hydro-decomposition method (Daengsakul et al., 2009). Calcium and cobalt acetates in a stoichiometric ratio were employed as starting ingredients. The starting materials were dissolved in deionized (DI) water. After completely dissolved, the mixed solution was heated up to 1053 K and held at that temperature for 6 h in a furnace under normal atmosphere. The obtained product was ground and calcined for a second time at 1123 K for 24 h. The calcined powder was

subjected to a ball-milling process using tungsten carbine balls with a diameter of 1.6 mm, a ball-per-powder ratio of 10:1, rotating speed of 300 rpm, milling time of 2.5 - 20 h and acetone as the dispersion media. The bulk ceramic of the milled powders was fabricated by a spark plasma sintering technique. More details can be found in the previous report (Prasoetsopha et al., 2013).

The $Ca_3Co_4O_{9+\delta}$ samples were characterized by X-ray diffraction (XRD) using an X-ray diffractometer with Cu-Kα radiation (Rigaku, UltimaIV). The morphology and chemical composition at the pressed and fractured surfaces of the samples were evaluated by a field emission scanning electron microscope (FESEM, JEOL, JSM 6500F) and energy dispersive X-ray spectroscopy (EDS), respectively. The sintered pellet was cut and polished in preparation for measuring its thermoelectric and transport properties. The resistivity and Seebeck coefficient were measured by using ZEM-3 (Ulvac-Riko) in a temperature range of 423-773 K. The thermal conductivity was calculated by $\kappa = DC_pd$, where D is the thermal diffusivity (measured using a laser flash technique, NETZSCH, LFA457), $C_p$ is the heat capacity (estimated from the Dulong-Petit model, $C_p = 3nR$, where $n$ is the number of atoms per formula unit and $R$ is the gas constant) and $d$ is the density of the sample, which were determined by using their mass and dimensions.

The crystallite sizes and lattice strain were calculated based on Scherrer's equation as follows:

$$d = \frac{0.9\lambda}{B\cos\theta} \tag{1}$$

$$B\cos\theta = \frac{0.9\lambda}{d} + \eta\sin\theta \tag{2}$$

where $d$, $\lambda$, $B$, $\theta$ and $\eta$ are the crystalline size, X-ray wavelength, line broadening at half the maximum intensity, Bragg angle and lattice strain, respectively.

## RESULTS AND DISCUSSION

### Phase identification and morphology

Figure 1 shows the XRD pattern of the unmilled powder, milled powder and sintered $Ca_3Co_4O_{9+\delta}$ samples. The unmilled and milled samples showed the single phase of $Ca_3Co_4O_{9+\delta}$ according to JCPDS card No. 21-0139. The intensities of the XRD peaks of the milled samples decreased with increasing milling time. This was probably due to a reduction in crystallite size (Table 1). Moreover, the lattice strains of the milled samples increased with increasing milling time. The longer milling time induced a larger number of defects in the crystal structure, which caused higher lattice strain. Highly dense bulk ceramics were obtained after spark plasma sintering (SPS) – 4.42 and 4.12 g/cm$^3$ for the unmilled and milled samples, respectively. However, the second phase of $Co_3O_4$ was observed from the bulk ceramics prepared from the milled powder. The impact of ball milling might create a small inhomogeneity distribution of Ca, Co and O, but cannot be detected by XRD. When we applied the SPS process, such inhomogeneity was

driven by a thermodynamic process – by the aid of heat and pressure – to form a more stable second phase that was detected in the XRD spectrum, as shown in Figure 1.

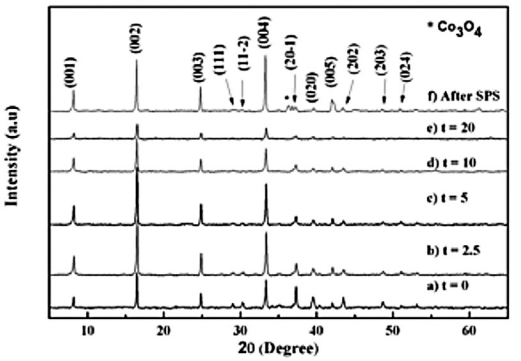


**Figure 1.** XRD pattern of $Ca_3Co_4O_{9+\delta}$ with various ball-milling times: a) t = 0 h, b) t = 2.5 h, c) t = 5 h, d) t = 10 h, e) t = 20 h and f) SPS bulk ceramics from milled powder with t = 2.5 h.

**Table 1.** Effect of milling time on particle size, crystallite size and lattice strain of $Ca_3Co_4O_{9+\delta}$ powders.

| Time, h | Particle size, nm | Crystallite size, nm | Lattice strain, % |
|---|---|---|---|
| 0 | 838 | 632 | 0.50 |
| 2.5 | 535 | 404 | 0.71 |
| 5 | 321 | 192 | 0.71 |
| 10 | 226 | 177 | 1.40 |
| 20 | 208 | 85 | 3.61 |

Figure 2 shows the SEM micrographs of the samples. The particle size of the sample was decreased from 1 μm (unmilled sample) to 200 nm (milled sample) by ball milling for 20 h, as shown in Figures 2 a) and 2 e), respectively. This implies that the ball-milling process can be used to reduce the particle size of $Ca_3Co_4O_{9+\delta}$. Not only did increased milling time decrease the particle size, but it also decreased crystallite sizes, based on the calculation of Scherrer's equation. Nevertheless, the SPS sample after milling for 2.5 h exhibited an impurity phase as can be seen at the fractured surface of the ceramic (black arrow of Figure 2 f). This result agreed with the XRD pattern (Figure 1), the surface morphology and the EDS data (Figure 3).

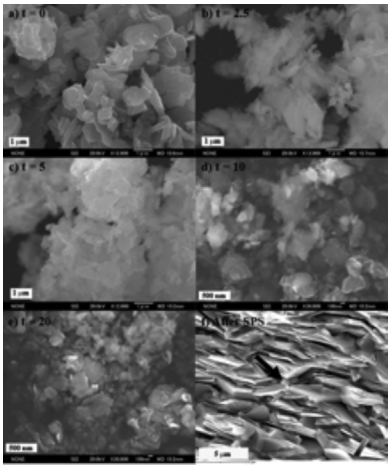


**Figure 2.** SEM micrograph of unmilled and milled $Ca_3Co_4O_{9+\delta}$ particles with various ball-milling times (a-e): a) t=0, b) t=2.5, c) t=5, d)=10, e) t=20 h; and fracture surface of f) t=2.5h after SPS. The black arrow indicates the impurity phase.

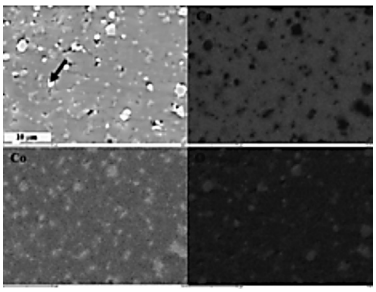


**Figure 3.** SEM micrograph of the pressed surface and the corresponding EDS mapping of the $Ca_3Co_4O_{9+\delta}$ ceramic. The black arrow points to the second phase.

Figure 3 shows SEM and EDS mapping of the SPS ceramics. The impurity phase is easily observed on the surface of bulk ceramic. Not only is the loss of Ca illustrated, but also the richness of Co and O are observed by EDS mapping. Moreover, the point analysis at the area of the second phase exhibited Ca:Co:O ratios of 7:25:67, which was significantly different from the ratio of the $Ca_3Co_4O_{9+\delta}$ phase.

**Thermoelectric properties**

Figure 4 shows temperature dependence of the Seebeck coefficient (S), resistivity (ρ) and thermal conductivity (κ). The S of the unmilled sample increased with increasing temperature, while the S of the milled sample first decreased with temperature to the minimum point at 573 K, and then increased with temperature. The non-monotonic feature of S for the milled sample can be explained by the

presence of the second phase ($Co_3O_4$). It has been reported that the S of $Co_3O_4$ varies with temperature, with a minimum point around 425 K (Ramachandran et al., 2011). In addition, it has been reported that $Co_3O_4$ enhanced the *S* in $Na_xCoO_2/Co_3O_4$ (Zhu et al., 2005). This could be the reason of the enhancement in *S* for the milled sample. On the other hand, the resistivity of both samples decreased with increasing temperature. The $\rho$ of the milled sample was higher than that of the unmilled samples. The higher $\rho$ of the milled samples may be a result of a reduction in crystallite size, which would enhance electron scattering at grain boundaries, and thus the increased $\rho$. The presence of the $Co_3O_4$ phase in the milled sample can also contribute to the increase of $\rho$, since $\rho$ of $Co_3O_4$ is much larger than that of $Ca_3Co_4O_{9+\delta}$ (Cheng et al.,1998; Sakamoto et al., 1997).

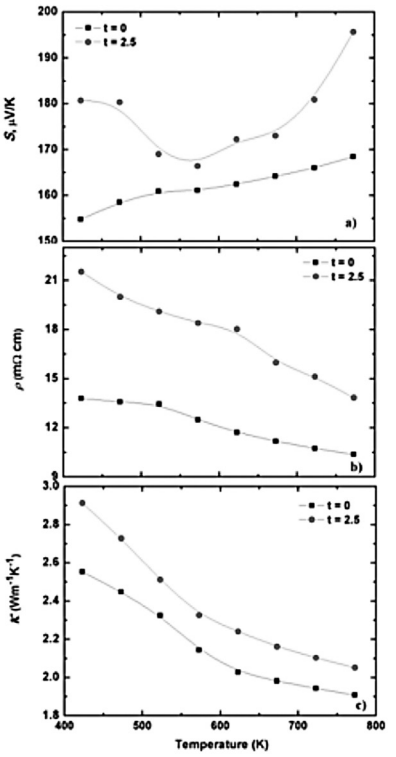


**Figure 4.** Temperature dependence of unmilled and 2.5 h milled $Ca_3Co_4O_{9+\delta}$: a) Seebeck coefficient, b) resistivity and c) thermal conductivity.

The thermal conductivity of the milled sample was higher than that of the unmilled sample (Figure 4c). This is unusual since the materials with smaller grain size should have the lower thermal conductivity, due to the stronger scattering of electrons at the grain boundary. However, in the case of $Ca_3Co_4O_{9+\delta}$, the major contribution of $\kappa$ is from phonon. We suspect that $\kappa$ of the second phase ($Co_3O_4$) is higher than that of $Ca_3Co_4O_{9+\delta}$, as in the case of another oxide (Koumoto et al., 2010). This can result in the increase in thermal conductivity of the milled sample. Nonetheless, this needs to be confirmed, since $\kappa$ of $Co_3O_4$ has not been

reported. Combining *S,* $\rho$ and $\kappa$, the *ZT* values of the unmilled and milled samples were calculated to be 0.11 and 0.10, respectively, at 773 K. The *ZT* of the milled sample did not change from the unmilled sample. If the impurity effect could be eliminated, different TE properties would occur.

In this study, we successfully synthesized polycrystalline $Ca_3Co_4O_{9+\delta}$ and used the ball-milling process to decrease the particle size. The longer the milling time, the smaller was the particle size. Unfortunately, the TE properties did not improve as expected, due to the presence of second phase formed during SPS.

## CONCLUSION

The particle size of $Ca_3Co_4O_{9+\delta}$ was reduced by a ball-milling technique. Milling for 20 h created a nanoparticle size of 200 nm. The bulk ceramic prepared from the milled powders of 2.5 h showed some impurity phase after the SPS process. The Seebeck coefficient, resistivity and thermal conductivity of the milled samples increased. The highest *ZT* of the milled sample was 0.10 at 773 K.

## ACKNOWLEDGMENTS

The authors would like to thank the Graduate School and Faculty of Science, Khon Kaen University for their financial support. This study was also supported by the Higher Education Research Promotion and National Research University Project of Thailand, Office of the Higher Education Commission, through the Advanced Functional Materials Cluster of Khon Kaen University.

## REFERENCES

Cheng, C.-S., M. Serizawa, H. Sakata, and T. Hirayama. 1998. Electrical conductivity of $Co_3O_4$ films prepared by chemical vapour deposition. Materials Chemistry and Physics 53 : 225.

Daengsakul, S., C. Mongkolkachit, C. Thomas, S. Siri, I. Thomas, V. Amornkitbamrung, and S. Maensiri. 2009. A Simple Thermal Decomposition Synthesis, Magnetic Properties, and Cytotoxicity of La0.7Sr0.3$MnO_3$ Nanoparticles. Applied Physics A: Materials Science & Processing 96 : 691. DOI: 10.1007/S00339-009-5151-0

Koumoto, K., I. Terasaki, and R. Funahashi. 2006. Complex Oxide Materials for Potential Thermoelectric Applications. Materials Research Society Bulletin 31 : 206.

Koumoto, K., Y. Wang, R. Zhang, A. Kosuga, and R. Funahashi. 2010. Oxide Thermoelectric Materials: A Nanostructuring Approach. Annual Review of Materials Research, 40 : 363. DOI: 10.1146/ANNUREV-MATSCI-070909-104521

Liu, C.-J., L.-C. Huang, and J.-S. Wang. 2006. Improvement of Thermoelectric Characteristics of Fe-doped Misfit-layered $Ca_3Co_4$-x$FexO_{9+\delta}$ (x = 0, 0.05, 0.1, and 0.2). Applied Physics Letters 89 : 204102. DOI: 10.1063/1.2390666

Liu, H. Q., Y. Song, S. N. Zhang, X. B. Zhao, and F. P. Wang. 2009. Thermoelectric Properties of $Ca_3$-x$YxCo_4O_{9+\delta}$ Ceramics. Journal of Physics and Chemistry of Solids 70 : 600. DOI: 10.1016/j.jpcs.2009.01.003

Masset, A. C., C. Michel, A. Maignan, M. Hervieu, O. Toulemonde, F. Studer, B. Raveau, and J. Hejtmanek. 2000. Misfit-layered Cobaltite with an Anisotropic Giant Magnetoresistance: $Ca_3Co_4O_9$. Physical Review B 62 : 166.

Nong, N. V., N. Pryds, S. Linderoth, and M. Ohtaki. 2011. Enhancement of the Thermoelectric Performance of p-type Layered Oxide $Ca_3Co_4$-x$GaxO_{9+\delta}$ Through Heavy Doping and Metallic Nanoinclusions. Advanced Materials 23 : 2484. DOI: 10.1002/adma.201004782

Noudem, J. G., D. Kenfaui, D. Chateigner, and M. Gomina. 2012. Toward the Enhancement of Thermoelectric Properties of Lamellar $Ca_3Co_4O_9$ by Edge-free Spark Plasma Texturing. Scripta Materialia 66 : 258. DOI: 10.1016/j.scriptamat.2011.11.004

Ohta, H., K. Sugirua, and K. Koumoto. 2008. Recent Progress in Oxide Thermoelectric Materials: p-type $Ca_3Co_4O_9$ and n-type $SrTiO_3$-. Inorganic Chemistry 47 : 8429. DOI: 10.1021/ic800644x

Pei, J., G. Chen, D. Q. Lu, P. S. Liu, and N. Zhou. 2008. Synthesis and High Temperature Thermoelectric Properties of Ca3.0-x-y$NdxNayCo_4O_{9+\delta}$. Solid State Communications 146 : 283. DOI: 10.1016/j.ssc.2008.03.012

Prasoetsopha N., S. Pinitsoontorn, A. Bootchanont, P. Kidkhunthod, P. Srepusharawoot, T. Kamwanna, V. Amornkitbamrung, K. Kurosaki, and S. Yamanaka. 2013. Local structure of Fe in Fe-doped misfit-layered calcium cobaltite: An X-ray absorption spectroscopy study. Jounal of Solid State Chemistry 204; 257. DOI: 10.1016/j.jssc.2013.05.038

Ramachandran, T., N. E. Rajeevan, and P. P. Pradyumnan. 2011. Thermoelectric Property of Cobalt Oxide Films. Solid State Physics: Proceedings of the 55$^{th}$ DAE Solid State Phaysics Symposium 2010 1349 : 1019. DOI: 10.1063/1.3606207

Sakamoto, S., M. Yoshinaka, K. Hirota, and O. Yamaguchi. 1997. Fabrication, Mechanical Properties, and Electrical Conductivity of $Co_3O_4$ Ceramics. Journal of American Ceramic Society, 80 : 267.

Shikano, M., and R. Funahashi. 2003. Electrical and Thermal Properties of Single-crystalline ($Ca_2Coo_3$)0.7$CoO_2$ with a $Ca_3Co_4O_9$ Structure. Applied Physics Letters 82 : 1851 -1853. DOI: 10.1063/1.1562337

Snyder, G. J., and E. S. Toberer. 2008, Complex Thermoelectric Materials. Nature Materials 7 : 105. DOI: 10.1038/nmat2090

Tritt, T. M., and M. Subramanian. 2006, Thermoelectric Materials, Phenomena, and Applications: A Bird's Eye View. Materials Research Society Bulletin 31 : 188. DOI: 10.4236/jamp.2014.210108

Wang, Y., Y. Sui, P. Ren, L. Wang, X. Wang, W. Su, and H. Fan. 2010. Strongly Correlated Properties and Enhanced Thermoelectric Response in $Ca_3Co_4$-x$MxO_9$ (M=Fe, Mn, and Cu). Chemistry of Materials 22 : 1155. DOI: 10.1021/cm902483a

Xiang, P.-H., Y. Kinemuchi, H. Kaga, and K. Watari. 2008. Fabrication and Thermoelectric Properties of $Ca_3Co_4O_9$/Ag Composites. Journal of Alloys and Compounds 454 : 364. DOI: 10.1016/j.jallcom.2006.12.102

Xu, L., F. Li, and Y. Wang. 2010. High-Temperature Transport and Thermoelectric Properties of $Ca_3Co_4$−x$TixO_9$. Journal of Alloys and Compounds 501 : 115. DOI: 10.1016/j.jallcom.2010.04.055

Yin, T., D. Liu, Y. Ou, F. Ma, S. Xie, J.-F. Li, and J. Li. 2010. Nanocrystalline Thermoelectric $Ca_3Co_4O_9$ Ceramics by Sol-gel Based Electrospinning and Spark Plasma Sintering. Journal of Physical Chemistry C 114 : 10061. DOI: 10.1021/JP1024872

Yuankui, C., C. Chuan, and L. Xiang. 2010. Effect on the Properties of Different Preparation Processes in $Ca_3Co_4O_9$ Thermoelectric Material. International Conference on Electrical and Control Engineering : 4672. DOI: 10.1109/ICECE.2010.1131

Zhu, P., T. Takeuchi, H. Ohta, W.-S. Seo, and K. Koumoto. 2005. Preparation and Thermoelectric Properties of $NaxCoO_2$/$Co_3O_4$ Layered Nano-Composite. Materials Transactions 46 : 1453. DOI: 10.2320/matertrans.46.1453